

Monitoring El Hierro submarine volcano with low and high resolution satellite images

F. Eugenio*^a, J. Marcello^a, J. Martin^a

^aInstitute for Oceanography and Global Change, Campus Universitario de Tafira,
35017 Las Palmas de Gran Canaria, Spain

ABSTRACT

Satellite remote sensing is providing a systematic, synoptic framework for advancing scientific knowledge of the Earth as a complex system of geophysical phenomena that, directly and through interacting processes, often lead to natural hazards. The recent eruption of a submarine volcano at the El Hierro Island has provided a unique and outstanding source of tracer that may allow us to study a variety of structures. The island off the Atlantic coast of North Africa—built mostly from a shield volcano—has been rocked by thousands of tremors and earthquakes since July 2011, and an underwater volcanic eruption 300 meters below sea level started on October 10, 2011. Thanks to this natural tracer release, low and high-resolution satellite images obtained from MODIS, MERIS and WorldView sensors have been processed to provide information on the concentration of a number of marine parameters: chlorophyll, phytoplankton, suspended matter, yellow substance, CDOM, particulate organic and inorganic, etc. This oceanographic remote sensing data has played, as well, a fundamental role during field campaigns guiding the Spanish government oceanographic vessel to the appropriate sampling areas. This paper illustrates the capabilities of satellite remote sensing systems to improve the understanding of submarine volcanic processes and hazards by providing more frequent observations and scientific information at a wide variety of wavelengths.

Keywords: Submarine volcano, El Hierro, remote sensing, oceanographic parameters, low-high resolutions satellite images

1. INTRODUCTION

After three months of volcanic unrest, characterized by more than 10,000 earthquakes (magnitude ≤ 4.3) and 5 cm of ground deformation, on October 10 2011 the National Seismic Network recorded a substantial decrease of seismicity together with continuous volcanic tremor, indicating the beginning of an eruptive phase. The impact caused by the underwater volcanic eruption, 300 meters below sea level, at the El Hierro Island (27.78N, -18.04W) has provided a unique and outstanding source of tracer that may allow us to study a variety of structures, as shown in Figure 1. The eruption is the first in the island chain in nearly 40 years and it is just off the southern coast of El Hierro. A milky green plume in the water stretched 25-30 kilometers at its widest and, approximately, 100 kilometers long, from a large mass near the coast to thin tendrils as it spreads to the southwest, as shown in the high resolution color composite images of RapidEye satellite of Figure 1 (d). The plume is likely a mix of volcanic gases and a blend of crushed pumice and seafloor rock.

Since then, regular multidisciplinary monitoring has been carried out in order to quantify the environmental impact¹. On October 24 2011, the Research Vessel Ramón Margalef of the Instituto Español de Oceanografía (IEO) carried out the first survey of the area, previously mapped in 1998 by the Spanish Research Vessel Hespérides. Comparison of present and 1998 bathymetry outlined a 700 m-wide, 100 m-high new volcanic cone resting at about 300 m depth. Monitoring submarine volcano is not an easy task compared with land volcano because it is covered by seawater and located in remote area.

Four months after it began, the underwater volcanic eruption off El Hierro Island persisted as shown in the natural-color satellite image (Figure 1 (e)), acquired on February 10, 2012 by the Advanced Land Imager (ALI) aboard the Earth Observing-1 (EO-1), that shows the site of the eruption, near the fishing village of La Restinga. Bright aquamarine water indicates high concentrations of volcanic material. Immediately above the location of volcano, a patch of brown water resembles a turbulent hot tub and indicates where the eruption is strongest.

*feugenio@dsc.ulpgc.es; phone +34 928 452979; fax +34 928 451243

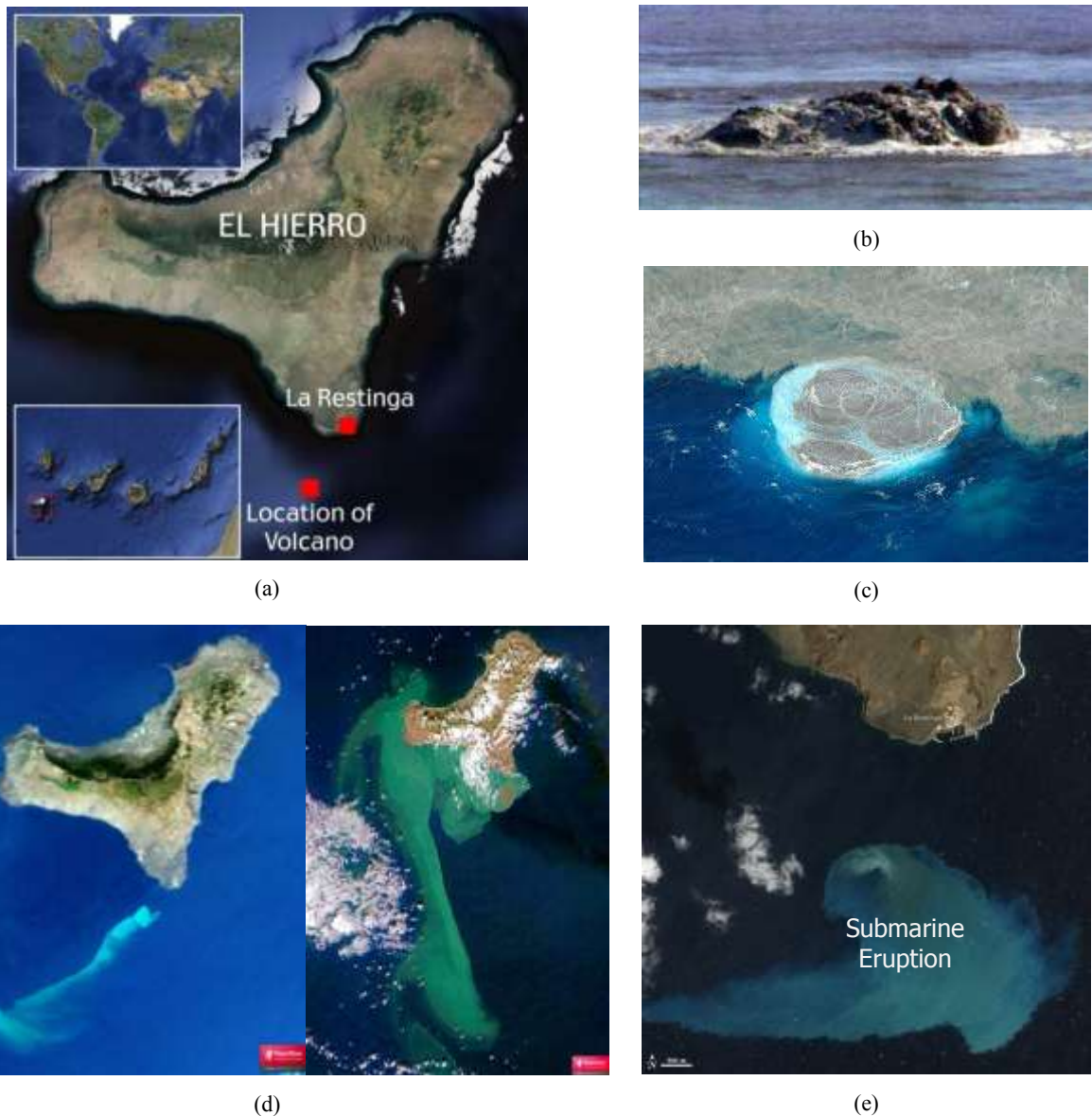


Figure 1. (a) El Hierro submarine volcano location (27.78N, -18.04W), (b) Strong degassing with abundant rock fragments generated large ‘bubbles’, some of them 10–15 m-high (8 November 2011), (c) Plumes of gas on ocean surface indicating a submarine eruptive fissure, (d) RAPIDEYE[®] color composite imagery acquired on October 26, 2011 and, (e) natural-color satellite image acquired by the Advanced Land Imager (ALI) aboard the Earth Observing-1 (EO-1) satellite (NASA[®]).

Satellite remote sensing technologies provide large amounts of data about the state and evolution of terrestrial environments. The usefulness of these data, collected to address particular problems at the Earth’s surface, depends on the capability to extract useful information on the processes of interest and to interpret them. Multitemporal and multi-satellite studies or comparisons between satellite data and local ground measurements require nowadays the establishment of a hierarchy of processes that allow the generation of operational products and the development of processing algorithms characterized by its precision, autonomy and efficiency. Satellite study of volcanoes is very useful because it can provide data for large areas of the Earth’s surface with a range of modalities ranging from visible to infrared, radar and beyond. Satellite sensing can also access remote locations and hazardous regions without difficulty. In this context, satellite remote sensing is a powerful tool for monitoring submarine volcanic activities such as discolored

seawater, floating material and volcanic plume. One issue with space-based volcano measurement is that atmospheric conditions (e.g. clouds) can interfere with many sensors (Visible, IR).

This paper illustrates the capabilities of satellite remote sensing systems to improve understanding of submarine volcanic processes by analyzing low and high resolution remote sensing images providing more frequent observations and scientific information at a wide variety of wavelengths. Thanks to this natural tracer release, low and high-resolution satellite images obtained from MODIS, MERIS and WorldView sensors have been processed to provide information on the concentration of a number of marine parameters: chlorophyll, phytoplankton, suspended matter, yellow substance, CDOM, particulate organic and inorganic, etc. This oceanographic remote sensing data has played, as well, a fundamental role during field campaigns guiding the Spanish government oceanographic vessel to the appropriate sampling areas.

2. SATELLITE REMOTE SENSING DATA

2.1 Remote Sensing Capabilities

The last two decades have witnessed the increasing use of remote sensing for understanding the geophysical phenomena underlying natural hazards. Observations from Earth orbiting satellites are complementary to local and regional airborne observations, and to traditional in situ field measurements and ground-based sensor networks in volcanology. The contributions of satellite remote sensing to Earth science, ranging from high-resolution topography (using e.g. Interferometric SAR, Lidar and digital photogrammetry) and geodesy to passive multispectral (such as ASTER, MODIS and WorldView2) and active microwave imaging, have transformed the discipline. This transformation has helped to define a rapidly growing field of applied research that increasingly will provide geospatial information products addressing the operational requirements of multi-hazard decision support tools and systems. Remote sensing data are contributing to comprehensive risk mitigation planning and improved disaster response².

Satellite remote sensing, in particular, is providing a systematic framework for scientific knowledge of the Earth. The key to understanding the Earth's dynamics and system complexity is to integrate observations at local, regional and global scales, over a broad portion of the electromagnetic spectrum with increasingly refined spectral resolution, spatial resolution and over time scales that encompass phenomenological lifecycles with requisite sampling frequency. Advances in computational science and numerical simulations are allowing the study of correlated systems, recognition of subtle patterns in large data volumes, and are speeding up the time necessary to study long-term processes using observational data for constraints and validation.

In the following sections, low and high satellite resolution remote sensing images obtained from MODIS, MERIS and WorldView2 sensors have been processed to obtain physical and biological oceanographic parameters that are being used to study and assess risks and effects due to El Hierro submarine volcano. This paper is not intended as a comprehensive treatment of the application of remote sensing to the selected natural hazards but rather as recognition of the contributions of satellite remote sensing to understanding underlying phenomena and providing critical information for decision support by emergency managers and the disaster response community. The intent is to raise awareness to the Earth scientific community about of the increasingly recognized potential of satellite remote sensing to assess the consequences of resultant changes, and the need for advanced observation platforms and monitoring systems for sustained measurements of the Earth relevant to disaster management.

2.2 Low resolution sensors

Satellite data from AQUA/TERRA-MODIS and ENVISAT-MERIS sensors have been the main source of image information to improve understanding of El Hierro submarine volcanic processes. The MODIS/MERIS instrument provides an excellent platform for volcanic activity detection and study, i.e., MODIS instruments flying on both the TERRA and AQUA satellites provides excellent temporal coverage with 2 daylight and 2 night overflights per 24 hours. In particular we have implemented a methodology for providing multitemporal/multisensor imagery information on the concentration of a number of oceanographic and biological parameters, specifically, chlorophyll, calcite and suspended matter data.

As indicated, MODIS (Moderate Resolution Imaging Spectroradiometer) is a key instrument aboard the TERRA (EOS AM) and AQUA (EOS PM) satellites. Terra's orbit around the Earth is timed so that it passes from north to south across the equator in the morning, while Aqua passes south to north over the equator in the afternoon. TERRA MODIS and AQUA MODIS are viewing the entire Earth's surface every 1 to 2 days, acquiring data in 36 spectral bands³. The MODIS spatial resolution are: 250 m (bands 1-2), 500 m (bands 3-7) and 1000 m (bands 8-36). These data improves our understanding of global dynamics and processes occurring on the land, in the oceans, and in the lower atmosphere. MODIS is playing a vital role in the development of validated, global, interactive Earth system models able to predict global change accurately enough to assist policy makers in making sound decisions concerning the protection of our environment.

On the other hand, MERIS, aboard ENVISAT satellite, is a programmable, medium-spectral resolution, imaging spectrometer operating in the solar reflective spectral range. Fifteen spectral bands can be selected by ground command⁴. One important capability of MERIS is providing full resolution (FR) data at 300 m resolution. The instrument scans the Earth's surface by the so called "push-broom" method. Linear CCD arrays provide spatial sampling in the across-track direction, while the satellite's motion provides scanning in the along-track direction. MERIS is designed so that it can acquire data over the Earth whenever illumination conditions are suitable. The instrument's 68.5° field of view around nadir covers a swath width of 1150 km. The principal contributions of MERIS data to the study of the upper layers of the ocean are: the measurement of photosynthetic potential by detection of phytoplankton (algae); the detection of yellow substance (dissolved organic material) and the detection of suspended matter (re-suspended or river borne sediments). Figure 2 shows, comparatively, the spectral bands of MERIS versus MODIS in VIS and Near IR bands.

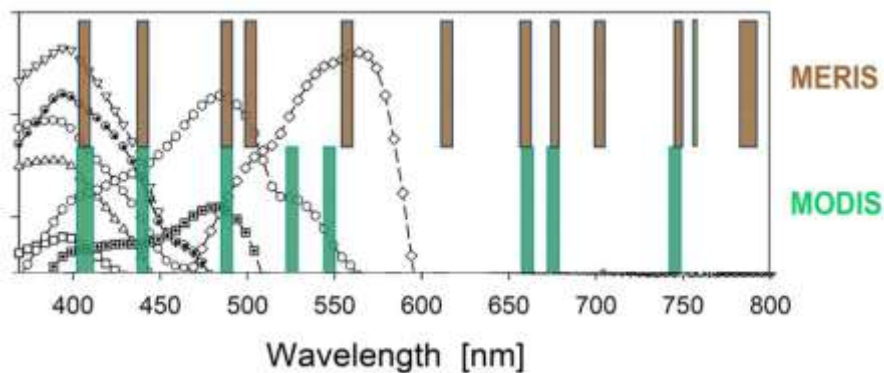


Figure 2. MERIS vs MODIS reflective spectrals bands.

MODIS delivered daily images of the study area while MERIS, with a longer revisit cycle, yielded an image every two–three days. Nevertheless, MERIS had a significant advantage over MODIS with respect to the estimation of biological parameters (i.e., chl- a concentration) due to its possession of a spectral band at 708 nm and its higher spatial resolution (260 m × 290 m compared to 1 km × 1 km for MODIS).

MODIS/MERIS oceanographic parameters

Phytoplankton biomass is an important bio-physical characteristic that is commonly used to assess the eutrophic status of water bodies. The photosynthetic pigment chlorophyll-a (chl-a) is a key indicator of phytoplankton biomass. Thus the estimation of chl- a concentration is critically integral to monitoring water quality. Photoactive pigments such as chl-a cause distinct changes in the color of water by absorbing and scattering the light incident on water. Chl-a concentration can be estimated from remotely sensed spectral reflectance data by relating optical changes observed in the reflected light at specific wavelengths to the concentration of chl-a.

For our study area, El Hierro submarine volcano, after the retrieval of remote sensing reflectance, the three-band model was applied to MODIS data (OC 3 algorithm) and the four-band models to MERIS data (OC4 algorithm) as follows⁵,

$$Chla \left(\frac{mg}{m^3} \right) = 10^{(0.2830 - 2.753 * x + 1.457 * x^2 + 0.659 * x^3 - 1.403 * x^4)}$$

$$x = \log \left(\max \left\{ \frac{R_{445}}{R_{555}}, \frac{R_{488}}{R_{555}} \right\} \right) \quad (1)$$

$$Chla \left(\frac{mg}{m^3} \right) = 10^{(0.3666 - 3.067 * x + 1.903 * x^2 + 0.649 * x^3 - 1.532 * x^4)}$$

$$x = \log \left(\max \left\{ \frac{R_{445}}{R_{555}}, \frac{R_{490}}{R_{555}}, \frac{R_{510}}{R_{555}} \right\} \right) \quad (2)$$

where R_x is the remote sensing reflectance at the waveband centered at x nm.

The Chl-a concentration results obtained by MODIS-OC3 and MERIS-OC4 algorithms due to El Hierro submarine volcano compared with RGB MODIS imagery are presented in Figure 3. As it can be observed in this particular multisensorial imagery of the same date, the eruption of the submarine volcano has led to a qualitative substantial variation de Chl-a concentration.

Coastal waters are often characterized by high concentrations of suspended organic and inorganic material derived from seabed resuspension or discharge of particle-laden rivers or in our study by the activity of submarine volcano. High concentrations of suspended materials directly affect many water column and benthic processes such as phytoplankton productivity, productivity of submerged aquatic vegetation, nutrient dynamics, the transport of pollutants and other materials. The distribution and flux of suspended sediments are highly variable in coastal environments and vary over a broad spectrum of time and space scales. This variability renders most traditional field sampling methods as inadequate in studies to resolve sediment dynamics in complex coastal waters. Consequently, there is considerable interest in the use of remotely sensed data to provide synoptic maps of suspended materials such as suspended sediments in coastal waters.

The MERIS-TSM (Total Suspended Matter) product (obtained from ESA) is defined to represent the concentration of total suspended particulates in gm^{-3} . The particulate backscatter at visible bands is deduced from the water-leaving reflectance spectrum and converted from optical units (backscatter in m^{-1}) to geophysical units (concentration in gm^{-3}) using a fixed conversion factor derived for measurements on water samples. Thus, for the present study a regional product is used from the MERIS water-leaving reflectance at 753 nm expressed by⁶,

$$SPM \left(\frac{g}{m^3} \right) = 422 * \frac{R_{753}}{0.187 - R_{753}} + 3.7 \quad (3)$$

where SPM is the suspended particulate matter (g/m^3) and R_{753} is the reflectivity in the range of 753 nanometers. MERIS SPM (TSM) product obtained by the use of a single red band centered at 753 nm, as expressed in Eq.3, is shown in Figure 3(d).

2.3 High resolution sensors

It is now possible to carry out, using collected data from very high resolution (VHR) satellites, many applications that in the recent past were exclusive to airborne and on site surveys. Due to the high geometrical resolution, the multi-spectrality, the high radiometric sensitivity, the revisit capabilities, the area imaged by a single frame or strip and to the accurate geometrical processing, that can be targeted. VHR imagery is a key source of information for a wide range of applications related to natural, semi-natural and urban up to desert environments.

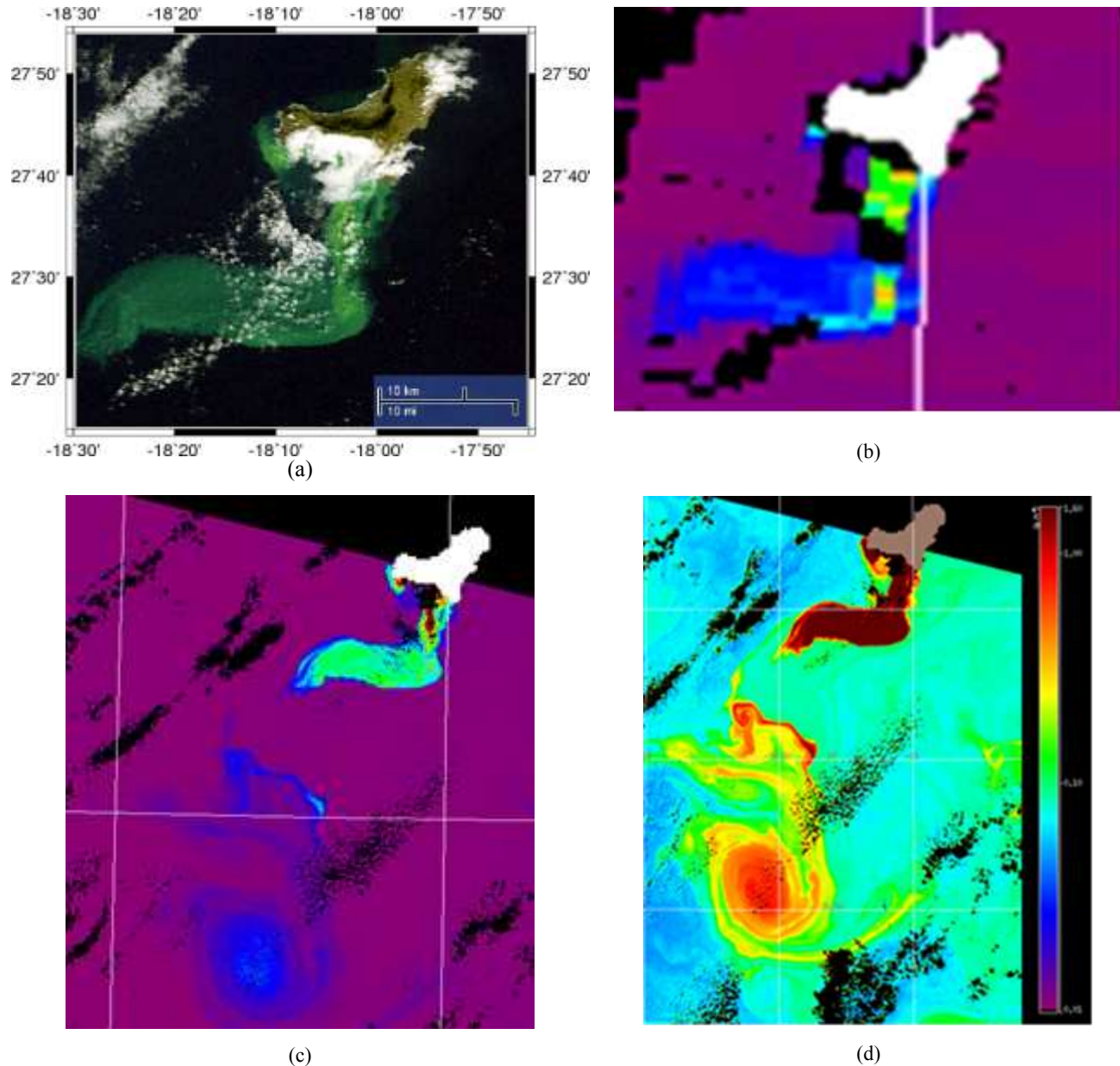


Figure 3. (a) MODIS/TERRA image (red: $0.66 \mu\text{m}$; green: $0.55 \mu\text{m}$; blue: $0.47 \mu\text{m}$) acquired over El Hierro submarine volcano area on November 9, 2011. The image shows a milky green plume in the water near the coast tendrils as it spreads to the southwest, (b) MODIS chlorophyll- a concentration obtained by OC3 algorithm (Eq. 1), (c) MERIS chlorophyll-a concentration obtained by OC4 algorithm (Eq. 2) and, (d) MERIS level 2 full resolution Total Suspended Matter (TSM) product showing a clear anticyclonic eddy (ESA[®]).

The WorldView-2 high-resolution commercial imaging satellite was launched on October 8, 2009, from Vandenberg AFB, and was declared to be operating at Full Capability on January 4, 2010. The satellite is in a nearly circular, sun-synchronous orbit with a period of 100.2 minutes, an altitude of approximately 770 km, and with a descending nodal crossing time of approximately 10:30 a.m. WorldView-2 acquires 11-bit data in nine spectral bands covering panchromatic, coastal, blue, green, yellow, red, red edge, NIR1, and NIR2, as shown in Figure 4. Each sensor is focused to a particular part of the electromagnetic spectrum to be sensitive to a specific type of feature on the ground or property of the atmosphere⁷.

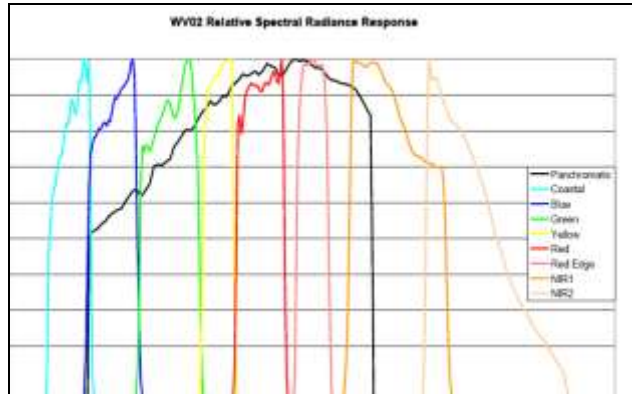


Figure 4. Spectral Response of the WorldView 2 panchromatic and multispectral imager.

This work relied on the Ortho Ready Standard Worldview-2 images. The covering place is part of the south of El Hierro Island. The images included 8 multispectral bands and one panchromatic band. At nadir, the collected nominal ground sample distance is 0.46 m (panchromatic) and 1.84 m (multispectral). However, commercially available products are resampled to 0.5 m (panchromatic) and 2.0 m (multispectral). The nominal swath width is 16.4 km. In Figure 5, a high resolution Ortho Ready Standard image acquired by WorldView-2 satellite in El Hierro submarine volcano area island is shown.

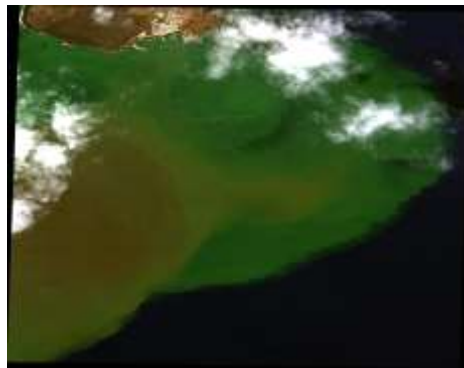


Figure 5. WorldView-2 color composite image acquired over El Hierro submarine volcano area on October 26, 2011. The image shows bright green water indicates high concentrations of volcanic material and a patch of brown water, in the volcano location.

The WorldView-2 satellite provides finer spatial resolution and more spectral information in the visible spectrum than previous satellites, positioning it as the forerunner for oceanographic parameters mapping. So, high-resolution satellite images obtained from WorldView-2 sensor have been processed to provide information on the concentration of chlorophyll and suspended matter in the El Hierro submarine volcano area. To obtain Chl-a concentration of, after the retrieval of remote sensing reflectance, the OC 3 algorithm (see Equation (1)) has been adapted to our study area. For turbidity parameter, the Case 1 suspended particulate material (TSM) concentration algorithm is a fine-tuning of Tassan's approach⁸. The Chl-a and TSM can be expressed by,

$$TSM \left(\frac{g}{m^3} \right) = 10^{1.83 + 1.26 \times \log \left(\frac{R_{555} + R_{670}}{(R_{490}/R_{555})^{-1.2}} \right)} \quad (4)$$

3. RESULTS

As mentioned, monitoring a submarine volcano is not an easy task compared with land volcano because it is covered by seawater and located in a remote area. By processing daily MODIS images aboard AQUA/TERRA satellites, in Figure 6, it can be observed the water turbidity variation during October 2011 due to the eruption of the submarine volcano (starting in October 12, 2011). The results obtained by multitemporal MODIS imagery have allowed the temporal monitoring of the milky green plume in the water stretched (approximately 25-30 kilometers at its widest and 100 kilometers long) from a large mass near the coast to thin tendrils as it spreads to the southwest.

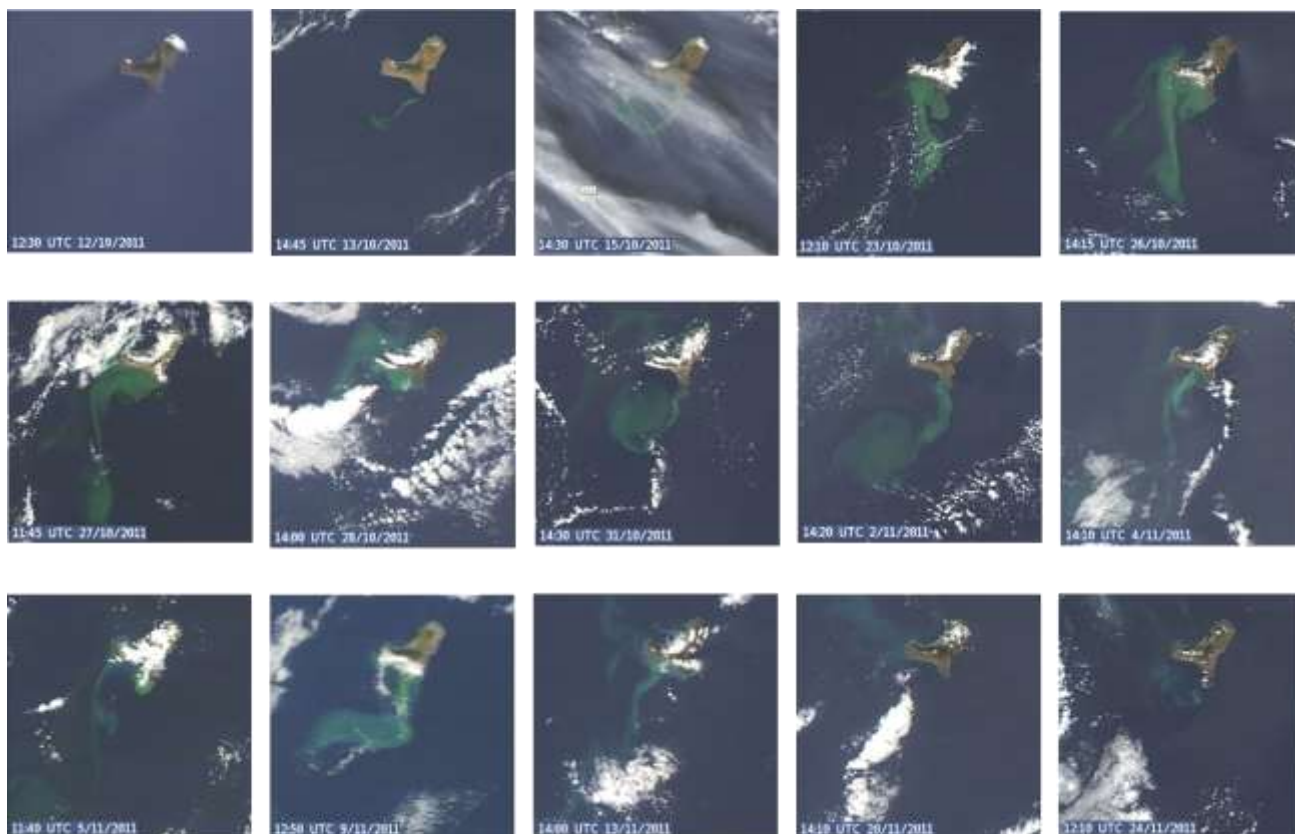


Figure 6. NASA MODIS RGB multitemporal images monitoring El Hierro submarine volcano (October, 2011).

The MODIS and MERIS models (equations (1)–(2)) gave reasonably close relationships with analytically measured chl-a concentrations. Among the different atmospheric correction procedures for MODIS data, in terms of the ability of the model to explain the highest percentage of the variation in chl-a concentration, any procedure stood out consistently better than the rest. Figure 7 and 8 show the chl-a concentration monitoring of the submarine volcano by multitemporal MODIS and MERIS imagery. Figure 7 shows the results from MODIS data for the three-band model OC3 (equation (1)). Figure 8 shows the results from MERIS imagery for data collected from the El Hierro island during the period 9–23 November 2011 for the four-band model OC4 (equation (2)). As illustrated, in general, the model values derived from MODIS/MERIS data show a great correlation between the chl-a concentration values obtained by MODIS data and the corresponding obtained by processing MERIS data (i.e., chl-a concentration showed in MODIS/MERIS images acquired on November 9, 2011).

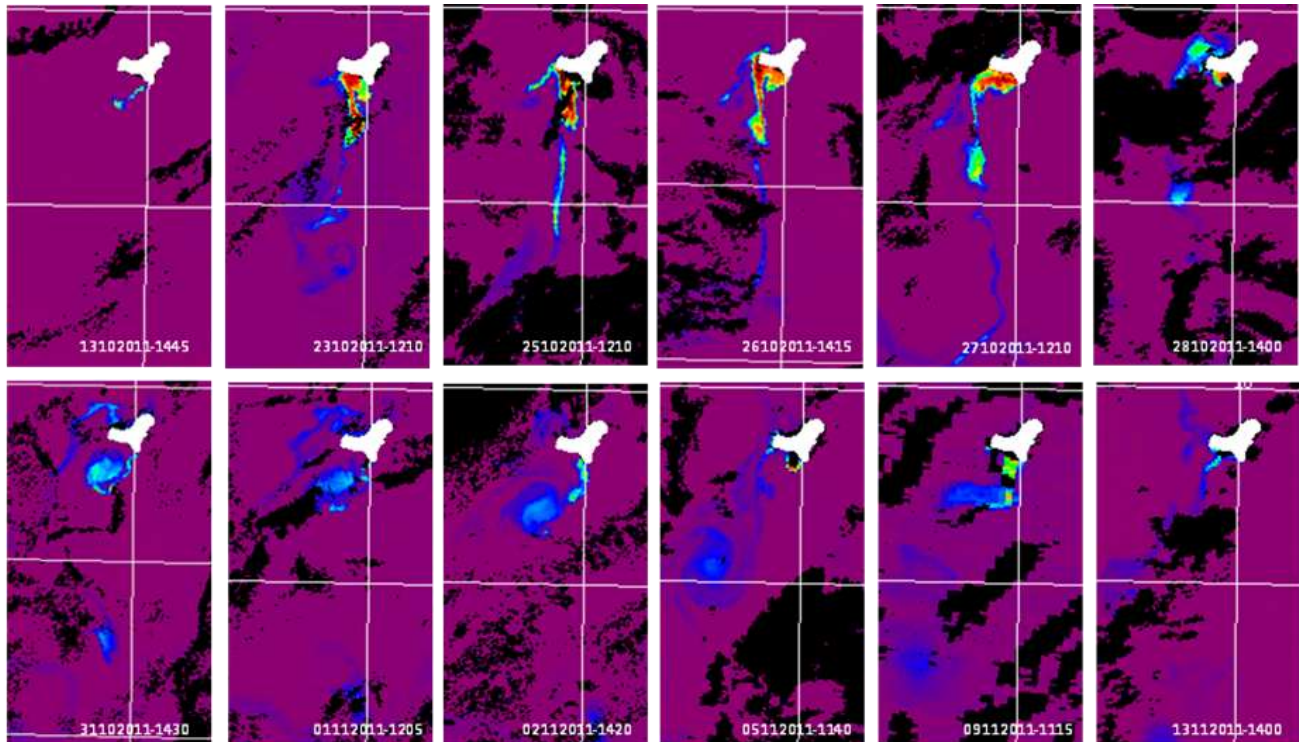


Figure 7. NASA-MODIS Chlorophyll concentration image sequence during the period 13 October–13 November 2011.

On the other hand, the present study looks qualitatively at the standard products for MERIS-TSM and the corresponding regional products. This analysis considered four images from November 2011, as shown in Figure 9. Comparison of the MERIS-TSM for these images shows similar qualitative patterns respect to MERIS Chl-a concentration, clearly related to corresponding patterns in the RGB image. The main difference is a systematically higher concentration of volcanic material, especially in the coastal waters near the location of submarine volcano. The disadvantages of MERIS, particularly for TSM mapping, are the reduced frequency (related to swath and sunglint) and availability of data.

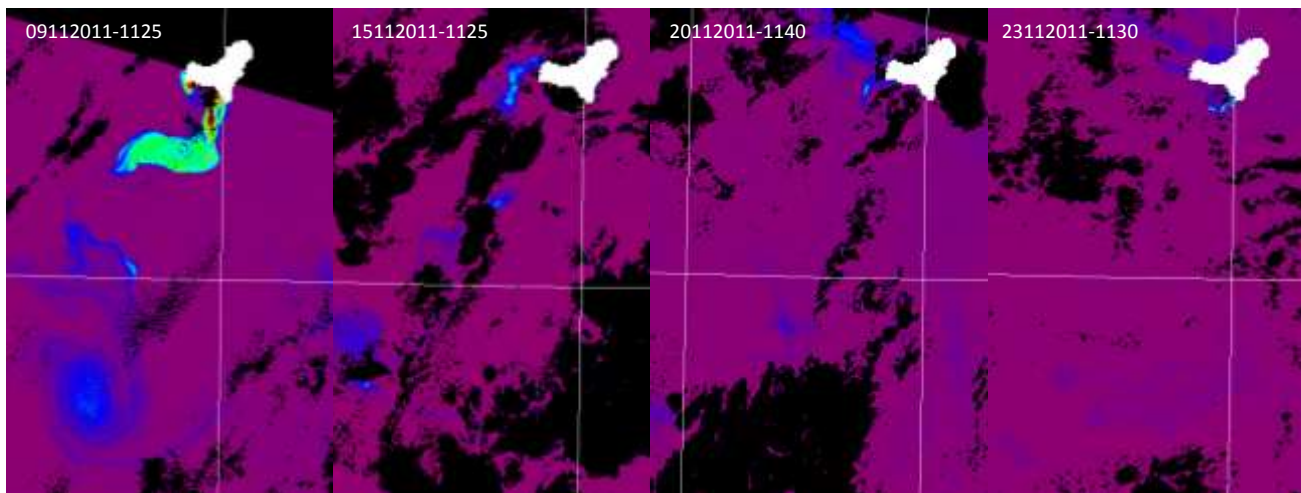


Figure 8. ESA-MERIS Chlorophyll concentration image sequence during the period 9–23 November 2011.

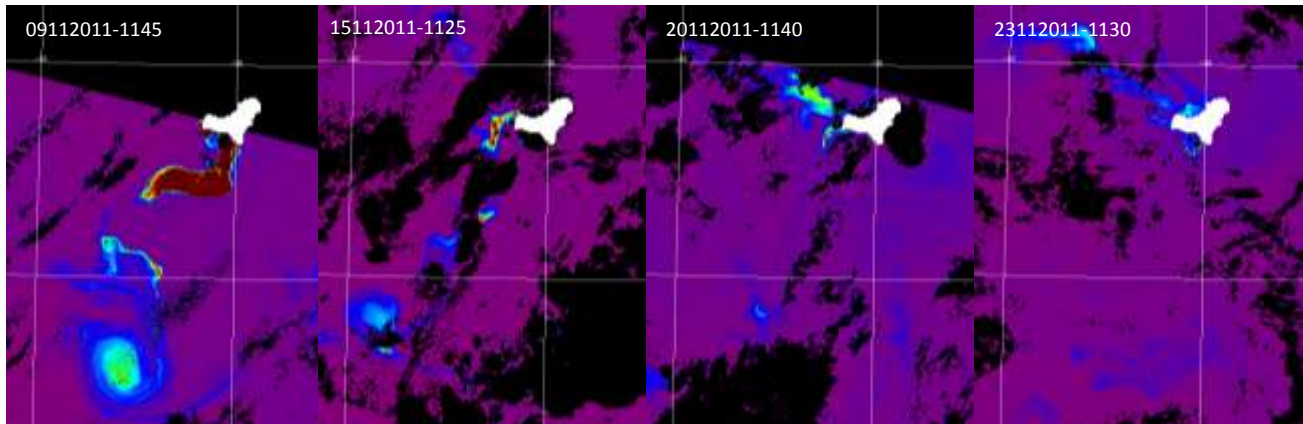


Figure 9. MERIS- TSM multitemporal images of El Hierro submarine volcano (9-23 November, 2011).

Finally, in order to check the proper functioning of the selected Chlorophyll concentration and Total Suspended Matter (TSM) algorithm in high-resolution images of the submarine volcano area, the WorldView-2 image (see Fig. 5) was radiometrically and atmospherically corrected and processed to obtain Chl-a and TSM oceanographic parameters. The results obtained are presented in Figure 10.

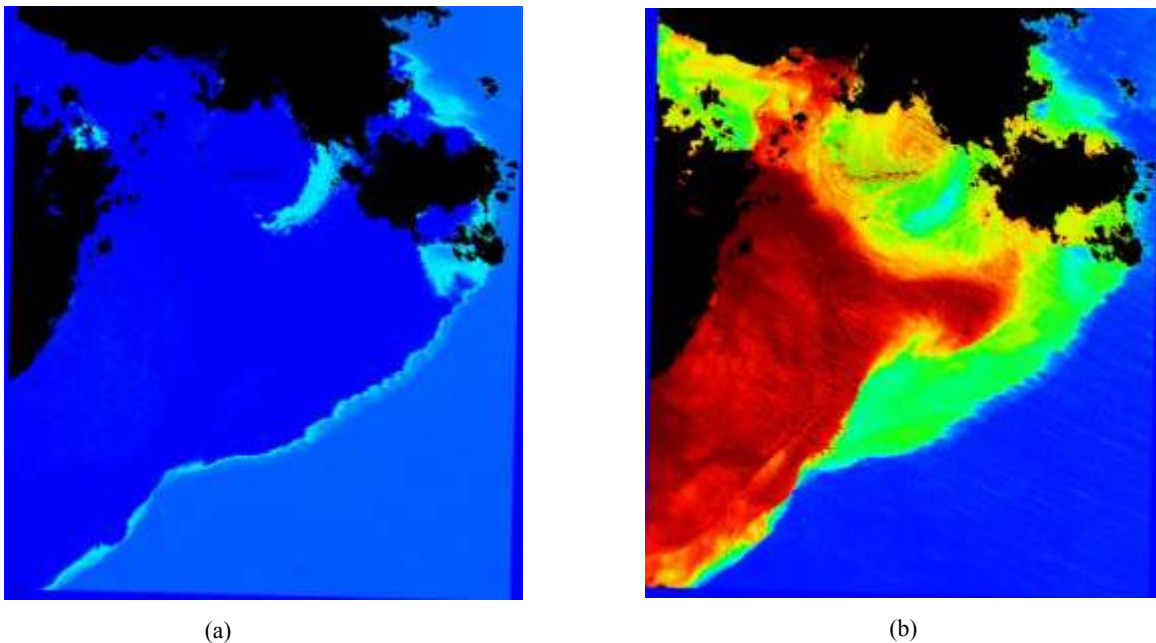


Figure 10. (a) WorldView-2 chlorophyll-a concentration obtained by the OC3 adapted algorithm and, (b) Total Suspended Matter (TSM) obtained by a fine-tuning of Tassan's algorithm.

4. CONCLUSIONS

The use of remote sensing for mapping and monitoring natural hazards has diversified in recent years owing to an increase in data availability and technological advances in their interpretation. Satellite remote sensing systems has proven useful for a range of applications including the capabilities to improve the understanding of submarine volcanic processes by analyzing low and high resolution remote sensing images providing more frequent observations and scientific information.

This paper describes an effort to integrate space-borne sensing data from MODIS (Terra and Aqua), MERIS and Worldview-2 to improve global volcano monitoring and to provide information on the concentration of two marine parameters: chlorophyll and suspended matter. This oceanographic remote sensing data has played, as well, a fundamental role during field campaigns guiding the Spanish government oceanographic vessel to the appropriate sampling areas.

Actually, researchers of the Physical Oceanography Department of IEO Centre in the Canary Islands along with researchers of the Chemistry Department of ULPGC, continue to study of the physical-chemical properties of the water around the submarine volcano of El Hierro Island. The scientists have observed an area of 500 meter of radius around the submarine volcanic cone where the physical-chemical properties of the water column are still significantly affected. This is the case of pH and salinity, which decrease 1.8 units and 0.1 below the normal values, respectively. In this context, we are going to investigate with low, medium and high resolution remote sensing satellite images the evolution of these physical-chemical parameters due to the submarine volcano.

The favorable results from this study have spawned a follow-up project that consists on the upgrade of the developed oceanographic techniques to study the submesoscale structures (i.e., as shown in Figure 3(d)) and their possible relationship with lateral mixing and biological effects, combining low, medium and high-resolution multisensor satellite images of El Hierro tracer with in situ observations, and implementing a surface motion model using optical flow algorithms applied in satellite image sequences.

ACKNOWLEDGEMENTS

This work has been supported by the Proyecto Estructurante de Teledetección (PET), ACIISI, Govern of Canary Islands and by the TELECAN project MAC/3/C181 (Programa de Cooperación Transnacional Madeira-Azores-Canarias 2007/2013). MERIS data used here was supplied by the European Space Agency under Project 10134.

REFERENCES

- [1] Fraile-Nuez, E. et al., "The submarine volcano eruption at the island of El Hierro: physical-chemical perturbation and biological response," *Scientific Reports*2, doi:10.1038/srep00486 (July, 2012).
- [2] Tralli D. M., Blom, R. G., Zlotnicki, V., Donnellan, A., Evans, D. L., "Satellite remote sensing of earthquake, volcano, flood, landslide and coastal inundation hazards," *ISPRS Journal of Photogrammetry and Remote sensing*, 59 (4), 185-198 (2005).
- [3] Isaacman, A., Toller, G., Guenther, B., Barnes, W. L. and Xiong, X., "MODIS Level-1B Calibration and Data Products," *Proc. SPIE Earth Observing Systems VIII*, 5151, 552-562 (2003).
- [4] European Space Agency, "MERIS Product Handbook," Issue 2.1 (October, 2006).
- [5] Moses, W. J., Gitelson, A., Berdnikov, S. and Povazhnyy, V., "Estimation of chlorophyll-a concentration in case II waters using MODIS and MERIS data—successes and challenges," *Environ. Res. Lett.* 4, 045005doi:10.1088/1748-9326/4/4/045005 (2009).
- [6] Ruddick, K., Park, Y. and Nechad, B., "MERIS imagery of Belgian coastal waters," *Proc. MERIS User Workshop, Frascati, Italy, 10 – 13 November 2003 (ESA SP-549, May 2004)*.
- [7] Updike, T. and Comp, C., "A Radiometric Use of WorldView-2 Imagery," *Technical Note* (2010).
- [8] Tassan, S., "Local algorithms using SeaWiFS data for the retrieval of phytoplankton, pigments, suspended sediment, and yellow substance in coastal waters," *Appl. Opt.*, 33, pp. 2369-2378 (1994).